J Fluoresc (2011) 21:793–801
DOI 10.1007/s10895-010-0772-4

ORIGINAL PAPER

Folate Conjugated CdHgTe Quantum Dots with High Targeting Affinity and Sensitivity for In vivo Early Tumor Diagnosis

Haiyan Chen · Li Li · Sisi Cui · Dider Mahounga · Jun Zhang · Yueqing Gu

Received: 5 July 2010 / Accepted: 1 November 2010 / Published online: 27 November 2010

Abstract CdHgTe-folate conjugates, acting as novel active-targeting fluorescence probes, were prepared by covalent conjugation of CdHgTe QDs and folic acid. Their characteristics, such as optical spectra, stability and cancer cell targeting were investigated in detail. The fluorescence wavelength of CdHgTe-folate conjugates was 790 nm and a full width at half-maximum (FWHM) of them was 50–70 nm. Their fluorescence stability could satisfy the need of long and continuous fluorescence imaging. The in vivo dynamic bio-distribution of CdHgTe-folate conjugates in S180 tumor beard mouse model was monitored by a NIR imaging system. The resultes indicated that CdHgTe-folate conjugates targeted to tumor effectively. The high fluorescence intensity together with targeting effect makes CdHgTe-folate conjugates promising candidates for imaging, monitoring and early diagnosis of cancer at molecular and cell level.

Keywords CdHgTe · Folate · Near infrared imaging · Cancer · Targeting

H. Chen · S. Cui · D. Mahounga · J. Zhang · Y. Gu
Department of Biomedical Engineering, School of Life Science and Technology, China Pharmaceutical University,
24 Tongjia Lane, Gulou District,
Nanjing 210009, China

L. Li
XinXiang College of Chemistry and Chemical Engineering,
Xinxiang University,
XinXiang City 453003, Henan Province, China

Y. Gu (✉)
China Pharmaceutical University,
Nanjing, China
e-mail: cpuyueqing@163.com

Introduction

The development of high-specific probes is of considerable interest in many research fields, from molecular to cellular biology and from molecular imaging [1, 2] to medical diagnosis [3, 4] and medical monitoring. As novel fluorescent probes, Quantum dots (QDs) overcome the intrinsic limitations of organic dyes and fluorescent proteins. They have unique optical and electric properties such as size and composition tunable fluorescence emission from visible to infrared wavelengths, narrow fluorescence emission band, long effective stokes shifts, high quantum yields and high level of photostability [5–7]. For their broad excitation profiles and narrow, symmetric emission spectra, QDs facilitate multicolor imaging feasible [8], in which multiple colors and intensities are combined to encode genes, proteins and small-molecule libraries [9, 10]. Moreover, QDs have the ability to conjugate with bio-recognition molecules such as peptides, nucleic acids, antibodies and small-molecule ligands for application as targeted fluorescent probes [11, 12]. Therefore, an important aspect of developing QDs in biomedical research is to utilize them as tumor diagnosis probes when they bind with tumor-targeting ligands, peptides, proteins, etc.

Tumor targeting for both therapeutic and diagnostic applications has been focused on some candidate ligands whose receptors are over-expressed in tumor cells [13–15]. One of such receptors is folate receptor (FR) [16], also known as the high affinity membrane folate-binding protein, a glycosylphosphatidylinositol (GPI)-linked membrane glycoprotein, preferentially mediates the uptake of exogenous folates and various derivatives into cell cytosol by endocytosis [17]. FR is over-expressed mainly on cancer cells, such as ovarian, bread, whereas its expression is at low levels in normal tissue [18, 19]. As a result, various folate conjugates have been prepared for targeted drug

delivery [20–22] and folate-mediated diagnosis [23–25]. Recently, in vivo early tumor diagnosis by NIR organic dyes-folate conjugate [23] or folate-nanoparticles (Au, magnetic nanoparticles) conjugate [26, 27] were reported, which have opened new possibilities for in vivo fluorescence imaging of tumor. However, conjugation of folate with NIR QDs and their application in early cancer diagnosis have not been reported, which will expand application field of NIR QDs.

In this study, CdHgTe QDs were covalently labeled with folate by coupling reagents (NHS/EDC). The optical properties of CdHgTe-folate conjugates were characterized. Immunocytochemical studies of CdHgTe-folate binding activity in cultured cancer cells was studied to confirm the affinity between FRs and CdHgTe-folate conjugates. In vivo dynamic distribution and tumor targeting of CdHgTe-folate were monitored by near-infrared fluorescence imaging system. Circulation of the CdHgTe-folate conjugate in mouse model was also addressed semi-quantitatively according to the time-dependent changes of fluorescence intensity.

Materails and Methods

Materials and Instruments

The reagent $Cd(NO_3)_2$ (AR) was purchased from Jinshanting new chemistry agents company (shanghai, China) and used directly without further purification. Tellurium powder (99.999%), $NaBH_4$, Thioglycolic acid (TGA), N-hydroxysulfo-succinimide (NHS) and 1-Ethyl-3 (3-dimethylaminopropyl) (EDC) were purchased from Guoyao chemistry agent corporation (Nanjing, China). Folate was purchased from Kaiji chemistry agent corporation (Nanjing, China). Water for all reactions and solution preparation was double distilled.

JEM-2100 transmittance electron microscope (Hitachi, Japan) was used to evaluate the morphology of particles. 754-PC UV-Vis spectrophotometer (Jinghua technological instrument corporation, Shanghai, China) was used for UV-Vis spectra measurement. S2000 eight-channel optical fiber spectrographotometer (Ocean Optics corporation, America), a HL-2000-HP-FHSA halogen lamp (filter: 560±30 nm, Ocean Optics corporation, America) and a NL-FC-2.0–763 laser (1=765.9 nm, nlight, China) light were utilized for fluorescence spectra detection

Synthesis of CdHgTe QDs and CdHgTe-Folate Conjugate

CdHgTe QDs was prepared following the method described previously [28]. In details, 0.092 g $Cd(NO_3)_2{\cdot}4H_2O$ was dissolved in 100 ml water, and 60 μl TGA (thiol stabilizer) was added under stirring, followed by adjusting the pH to 11.4–11.8 through drop-wise addition of 0.1 M NaOH. The solution was placed in a three-necked flask and O_2 was removed upon bubbling N_2 for 30 min. Under stirring, 600 μl of freshly prepared NaTeH solution (generated by the reaction of Te powder, $NaBH_4$ and water under N_2 atmosphere) was added into the reaction system. Before refluxing, a 5 μl $Hg(NO_3)_2$ saturated solution was added under nitrogen atmosphere over 30 min, which contributed to the red-shift of QDs to near infrared range. CdHgTe precursors were formed at this stage, accompanied by the solution color changing to brown. The precursor has an absorption spectrum in NIR region but no luminescence. The precursors are converted to CdHgTe QDs by refluxing for 2 h at 100°C under open-air conditions.

Folate was covalently conjugated with CdHgTe QDs by coupling agents (EDC/NHS). Carboxylic acid functional groups on the surface of CdHgTe QDs were activated by NHS and EDC. Briefly, 8.0 mg NHS and 5.0 mg EDC were dissolved in 0.50 ml water, and then dispersed in 3.0 ml CdHgTe aqueous solution for stirring 2 h. 3.0 mg folate was dissolved in 0.50 ml water by adjusting pH to weak alkaline. CdHgTe-folate conjugates were obtained by adding folate solution into the activated solution of CdHgTe QDs. The mixture reacted for 12 h under stirring at room temperature. To remove the excess of folate and coupling reagents (EDC/NHS) after reaction with QDs, the reaction solution was dialyzed (3 kDa cut-off) for 3 days in basic aqueous solution with fresh solution being changed five times each day.

Characterization of CdHgTe-folate Conjugate In vitro

Fourier Transform Infrared (FTIR) Study

To characterize the preparation of CdHgTe QDs-Folate conjugates, the IR spectra of CdHgTe QDs and CdHgTe-folate conjugates were measured by a FTIR 8400s Spectrometer (Shimadzu, Japan), respectively.

Transmission Electron Microscopy (TEM) Characterization

TEM images were performed on a Philips FEI Tecnai G2 20 S-TWIN instrument. Briefly, a diluted solution of CdHgTe-folate conjugates was dropped onto a 400-mesh carbon-coated copper grid with the excessive solvent immediately evaporated before being loaded into the microscope for observation.

Absorbance Spectra and Emission Spectra of CdHgTe-folate Conjugate

Absorbance spectra of CdHgTe-folate conjugates and CdHgTe QDs were measured by UV–visible spectrophotometer. Fluorescence spectra of CdHgTe-folate conjugate

and CdHgTe QDs were measured at room temperature using a S2000 eight-channel optical fiber spectrophotometer equipped with a halogen lamp.

Photostability of CdHgTe-folate Conjugates

To investigate photostability of CdHgTe-folate conjugates, CdHgTe-folate aqueous solutions were continually irradiated by a laser (1=765.9 nm, light intensity=26 mw). The fluorescence intensity of the samples were dectected at different time intervals within 150 min by a S2000 eight-gap optical fiber spectrographotometer

MTT assay of CdHgTe-folate Conjugates

Resistance to CdHgTe-folate conjugates was examined using the MTT assay. Briefly, A549 cells (Human Non-small Lung Cancer Cell Line) were seeded in a 96-well plate at a density of 5,000 cells/well on the day before the addition of the conjugates. CdHgTe-folate conjugates were incubated with cells in A549 cell culture medium in a cell culture incubator. The survival rates of A549 cells at 24 h after conjugates incubation were measured by MTT assay. After 3 h incubation at 37°C, the MTT working solution was removed. Then 200 μL DMSO was added into each well and the plate was shaken for 20 min at room temperature. All samples were assayed in triplicate and the survival rate was calculated as follows: Survival rate = (mean absorbance of test wells − mean absorbance of medium control wells)/(mean absorbance of untreated wells − mean absorbance of medium control wells) × 100%.

Cancer Cell Studies

To evaluate the optical properties of these particles in vitro, HeLa cells were incubated with CdHgTe QDs (0.1 mM) and CdHgTe-folate conjugates (0.1 mM) for 6 h at 37°C, respectively. After incubation, HeLa cells were washed with phosphate buffer saline for 3 times to remove any unbounded CdHgTe-folate conjugates and CdHgTe QDs. Fluorescence images of HeLa cells were collected by NIR fluorescence imaging system.

In vivo Fluorescence Imaging

S180 carcinosarcoma tumors were inoculated in the right flank area of Kunmin mice by the introduction of S180 cancer cells from a subcutaneous injecting, and the tumors were palpable in approximately 7 days. S180 tumor beard mice were denuded by a mixture of Na_2S (5%) and starch, daubing camphor ice immediately to avoid further skin erosion. The denuded mouse was put back to the animal house and ready for experiment after 24 h. All experiments were carried out in compliance with the guide for the care and use of laboratory animals in China Pharmaceutical University.

In a typical experiment, each mouse was anesthetized with an intraperitoneal (IP) injection of 150 μL ethyl carbamate (20 mg/ml) and then immobilized in a Lucite jig. CdHgTe-folate aqueous solution was injected through the tail vein into the mouse. NIR fluorescence imaging was then performed in a dark room on the mice by using NIR fluorescence imaging system. The light intensity of laser light from the fiber bundle was adjusted at 26 mw. For each mouse, background image (prior to injection) was firstly collected. A series of images were then collected at 1, 5, 30 min, 1, 2 and 5 h post-injection. The semi-quantitative study of the dynamic distribution of CdHgTe-folate conjugate in different tissues can be obtained by selecting the specific region of interest from the obtained images. The subjected mouse was then scarified, and different organs were separated, washed by natural saline and put together for fluorescence imaging.

Results

Identification of CdHgTe-folate Conjugates

A synthetic scheme of CdHgTe-folate conjugates is diplayed in Fig. 1, which demonstrates the conjugation principle in detail. Figure 2 shows the FTIR spectra of CdHgTe QDs (Fig. 1(a)) and CdHgTe-folate conjugate (Fig. 2(b)). The characteristic peaks of folate are the main difference between CdHgTe QDs and CdHgTe-folate conjugates. As shown in Fig. 2(a), the characteristic peaks at 3,414 and 1,582 cm-1 correspond to the O-H stretching vibration and >C=O stretching vibration of carboxylic acid groups in CdHgTe QDs. After folate conjugated with the QDs, two characteristic peaks (3,466 and 3,416 cm^{-1}) appeared in the range of 3,500 to 3,200 cm^{-1}, which corresponded to the N-H stretching vibration and the O-H stretching vibration of folate, respectively (Fig. 2(b)). Infrared peaks of 1,761 and 1,636 cm^{-1} correspond to the >C=O stretching vibration, which are different from the peaks in CdHgTe QDs due to the changing of the -COOH groups to –CONH- groups. The peaks in the range of 900 to 700 cm^{-1} are due to the bending vibration of C-H in benzene rings. These details indicate that folate have conjugated with CdHgTe QDs.

Size and Morphology

The size and morphology of CdHgTe-folate conjugates were investigated by high resolution TEM. The TEM images show that the conjugates have a uniform size and regular shape (Fig. 3 (a)). The average size of the nanocrystals based on the TEM

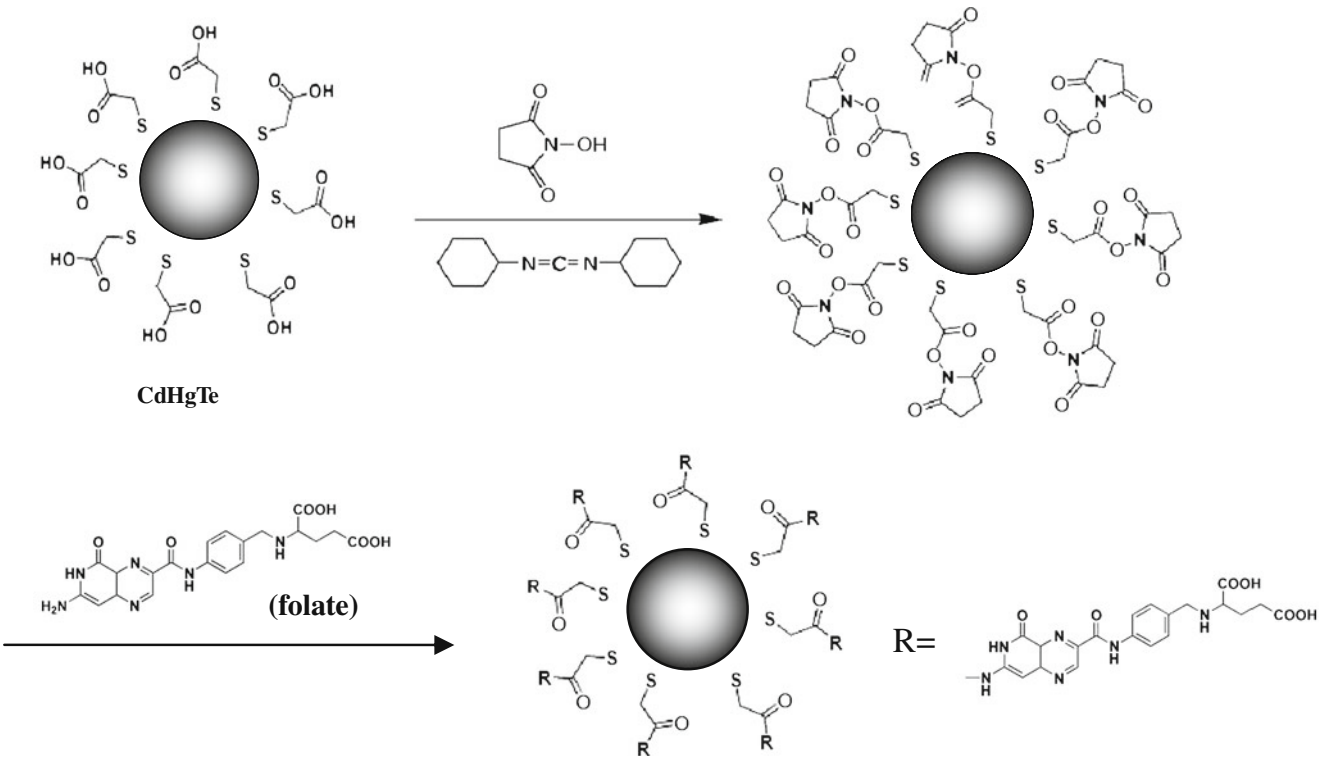

Fig. 1 A synthetic scheme of CdHgTe-folate conjugates

scale is 6.68 nm. As shown in the HRTEM image (Fig. 3(b)), the CdHgTe-folate conjugates are mono-dispersed and have a good crystal structure. Compared to the TEM images of CdHgTe QDs that were reported by our group [28], we could found that the size and morphology of these particles are not affected by the coupling of folate significantly.

Absorption and Emission Spectra

Figure 4(a) shows UV-Vis absorption spectra of CdHgTe-folate conjugates and CdHgTe QDs. A clearly resolved absorption maximum of the first electronic transition of CdHgTe QDs appears at 730 nm. After conjugating with folate, the absorption peak maintains at 730 nm and the shape of absorption peak retains as well. Figure 4(b) represents fluorescence spectra of CdHgTe-folate conjugates and CdHgTe QDs. For CdHgTe-folate conjugates, fluorescence peak appears at 790 nm which is the same as CdHgTe QDs precursor. Moreover, CdHgTe-folate conjugates hold strong fluorescence intensity as well as narrow full width at half-maximum (FWHM) of 50–70 nm.

Photostability

Photostability of CdHgTe-folate conjugates in aqueous solution was measured by irradiation with 765 nm laser light for 150 min. The fluorescence intensity of CdHgTe-folate conjugates increased a bit from 2,500 to 3,000 when irradiation time of laser light (765 nm) extended to 150 min (data was not shown), which suggested excellent stability of CdHgTe-folate conjugate in aqueous solution.

Cytotoxicity Studies of CdHgTe-folate Conjugates

To evaluate the biocompatibility of CdHgTe-folate conjugates as imaging probes, we investigated the cytotoxicity

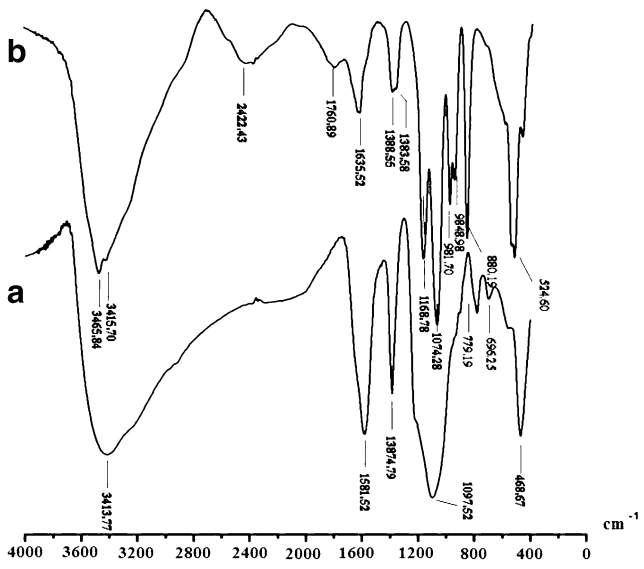

Fig. 2 **a** FTIR spectra of CdHgTe QDs; **b** CdHgTe-folate conjugate

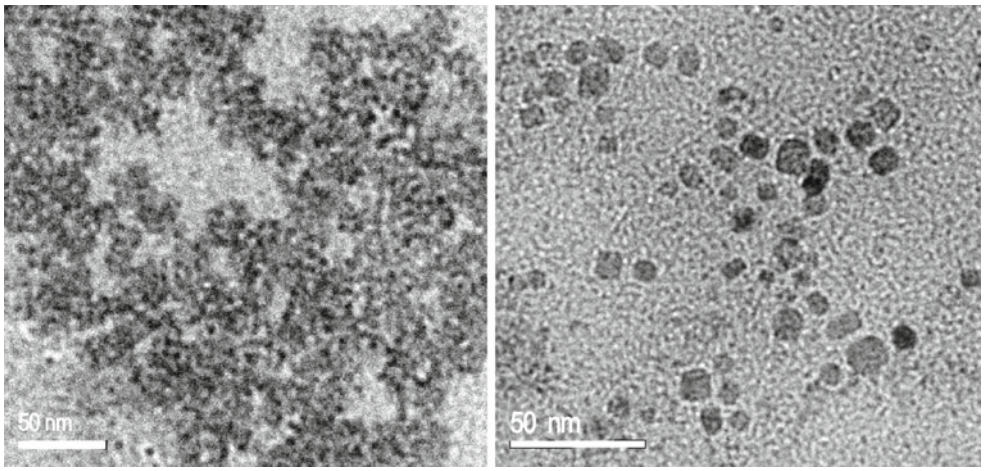

Fig. 3 **a** TEM image of CdHgTe-folate conjugate; **b** HRTEM image of CdHgTe-folate conjugate

of CdHgTe-folate conjugates using the MTT assay. The MTT assay relies on the mitochondrial activity of cells and represents a parameter for their metabolic activity. Figure 5 demonstrates a dose-dependent reduction in MTT absorbance for cells treated with CdHgTe-folate conjugates. After having been incubated for 24 h, CdHgTe-folate conjugates caused a minor reduction in cell viability (as high as 90%–100%) at lower dose. However, the conjugates caused a significant reduction (about 45% of control) in cell viability and exhibited cytotoxicity towards A459 cells at high dose (1.4 mM).

HeLa Cells Studies

CdHgTe-folate conjugates incubated with HeLa cells (FRs positive) for 6 h resulted in a significant uptake of conjugates into cells. Compared with CdHgTe QDs, higher fluorescence signals were observed for CdHgTe-folate conjugates incubated HeLa cells, which was shown in Fig. 6. Due to the non-uniformity of the laser intensity at a certain extent, the different fluorescence intensity of the plate lines were observed. In addition, fluorescence signals only appeared at the edge of the well. This phenomenon is attributed to edge effect in cell culture, which is more significant in the cell experiments treated with 96-well plates.

Tumor Targeting

Figure 7 represents a series of in vivo images detected by NIR fluorescence imaging system at different time interval. The fluorescent background prior to injection was firstly collected (Fig. 7(a)). After CdHgTe-folate conjugates was injected through the tail vein, fluorescence images of the mouse were collected at 1, 5, 30 min, 1, 2 and 5 h, respectively. The images indicated that CdHgTe-folate conjugates immediately distributed to the whole body by blood circulation after injection. Figure 7 (b) showed that these conjugates arrived at liver tissue in 10 s. As early as 5 min, fluorescence signal was observed in the tumor (Fig. 7(c)). During the next several time intervals, there was an obvious increase area of fluorescence signal in tumor site (Fig. 7 (d-f)).

To validate the information collected from in vivo fluorescence images, the mice were sacrificed and performed a thoracotomy. Figure 7(g) and (h) showed fluorescence image of the thoracotomy mouse at the corresponding time of Fig. 7(f). Fluorescence signals appeared in tumor and surrounding vessels, which was consistent with the fluorescence image shown in Fig. 7(f). Then, the major organs (liver, heart, spleen, kidney, intestine and lung) and tumor of the mouse were separated and the fluorescence image was acquired, which was shown in Fig. 7(i) and (j). Fluorescence intensity in liver, spleen and tumor tissues was strong enough to be distinguished from other tissues (heart, kidney, intestine and lung).

Due to the spectral characteristics of the CdHgTe-folate conjugates and the sensitivity of the instruments, NIR imaging technique is feasible to perform pharmacokinetic analysis. The dynamic changes of CdHgTe-folate conjugates in different organs/tissues can be acquired by selecting the specific region of interests (ROIs) from the obtained images. Figure 8 indicated analyzed data of CdHgTe-folate conjugates from tumor as well as liver. In each case, the background fluorescence that was measured before injection of the conjugates was subtracted. The fluorescence intensities in ROIs for tumor and liver tissues were averaged and then plotted against with the time, which is shown in Fig. 4. The elimination of folate-QDs conjugates from tumor and liver tissue was fitted with

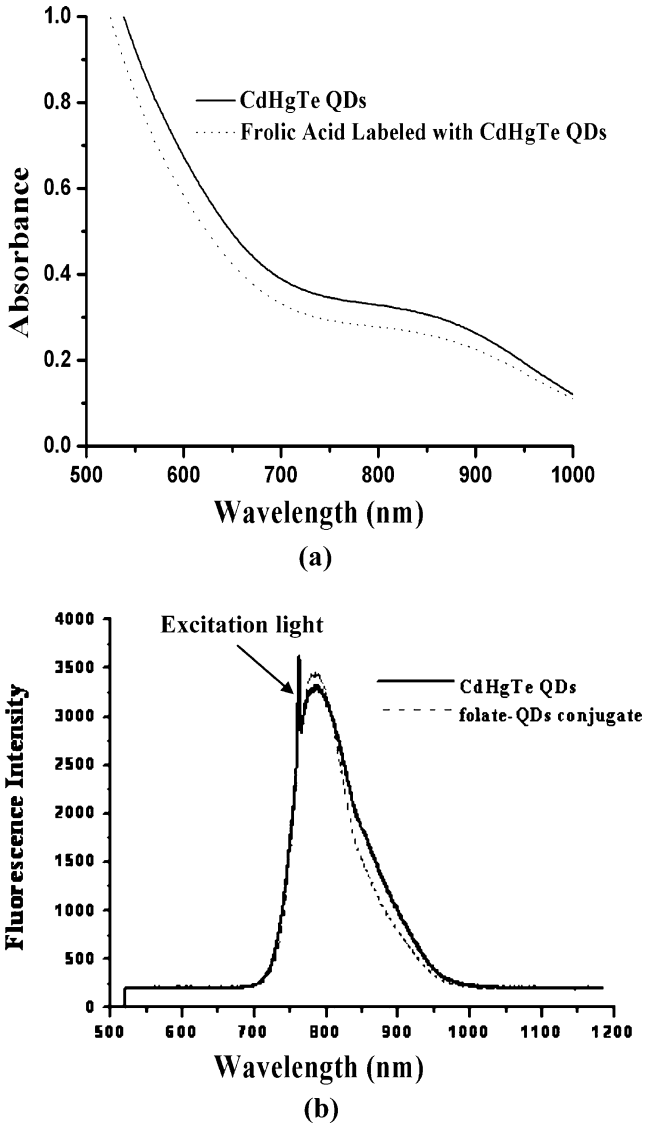

Fig. 4 **a** UV-Vis absorption spectra of CdHgTe-folate conjugates and CdHgTe QDs; **b** fluorescence spectra of CdHgTe-folate conjugates and CdHgTe QDs

polynomial forms, $y = 208.63 + 0.11x - 9.50e-4x^2 + 1.41e-6x^3$, $R^2 = 0.7853$ and $y = 87.84 + 1.39x - 0.01x^2 + 1.76e-5x^3$, R^2=0.7819 for each one.

Discussion

In this study, the application of CdHgTe-folate conjugates for in vitro cancer cell labeling and in vivo tumor-targeting imaging were reported. Highly luminescent and photostable thiol-capped CdHgTe NIR QDs were prepared in aqueous solution. TGA, a kind of weak acid, ionized in alkaline condition and thus enhanced the water dissolubility of CdHgTe QDs due to the surface of QDs coating with TGA.

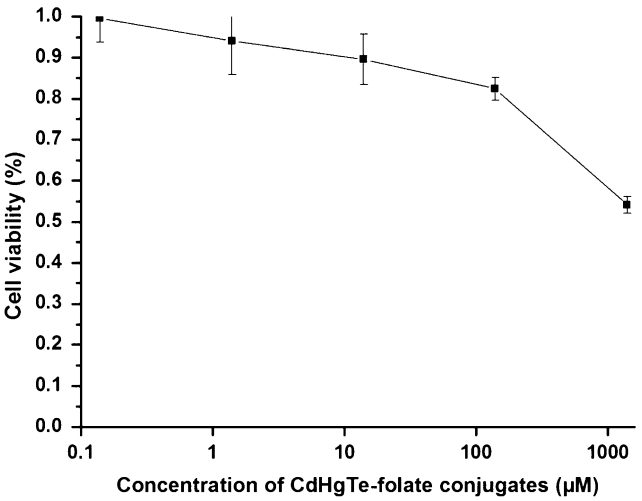

Fig. 5 Cytotoxicity studies of A549 cells treated with CdHgTe-folate conjugates. MTT assays illustrating cell viability upon exposing the cells with different concentration of CdHgTe-folate conjugates for 24 h

By varying the ratio of Hg composition and refluxing time, the emission wavelengths of these QDs could be tuned to 780~900 nm to avoid absorption and scattering signals of tissues in living animals.

CdHgTe-folate conjugates were successfully synthesized by using coupling agents NHS/EDC. The carboxylic groups on the surface of CdHgTe QDs were activated and conjugated with amino group of folic acid by covalent binding, which was confirmed by the FTIR spectra of CdHgTe QDs and CdHgTe-folate conjugates.

In order to investigate the influence on CdHgTe QDs after labled with folic acid, UV-Vis and fluorescence spectra were utilized for which are commonly used in the study of the structure and optical properties of QDs. UV-Vis and fluorescence spectra of CdHgTe-folate conjugates and CdHgTe QDs confirmed that these conjugates maintained the optical properties of CdHgTe QDs during the surface labeling process. The result indicated that CdHgTe QDs surface binding with folic acid might not change the interior structure of these QDs. Emission of QDs at visible range is not optimal for in vivo imaging because of the poor tissue

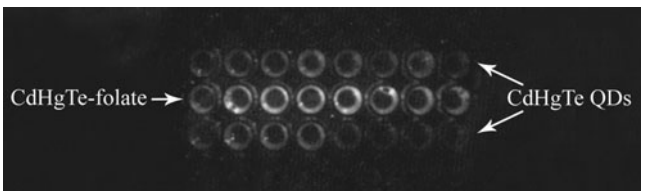

Fig. 6 Cancer cell binding activity study: CdHgTe-folate conjugates and CdHgTe QDs were incubated with HeLa cells (FRs positive) for 6 h, respectively

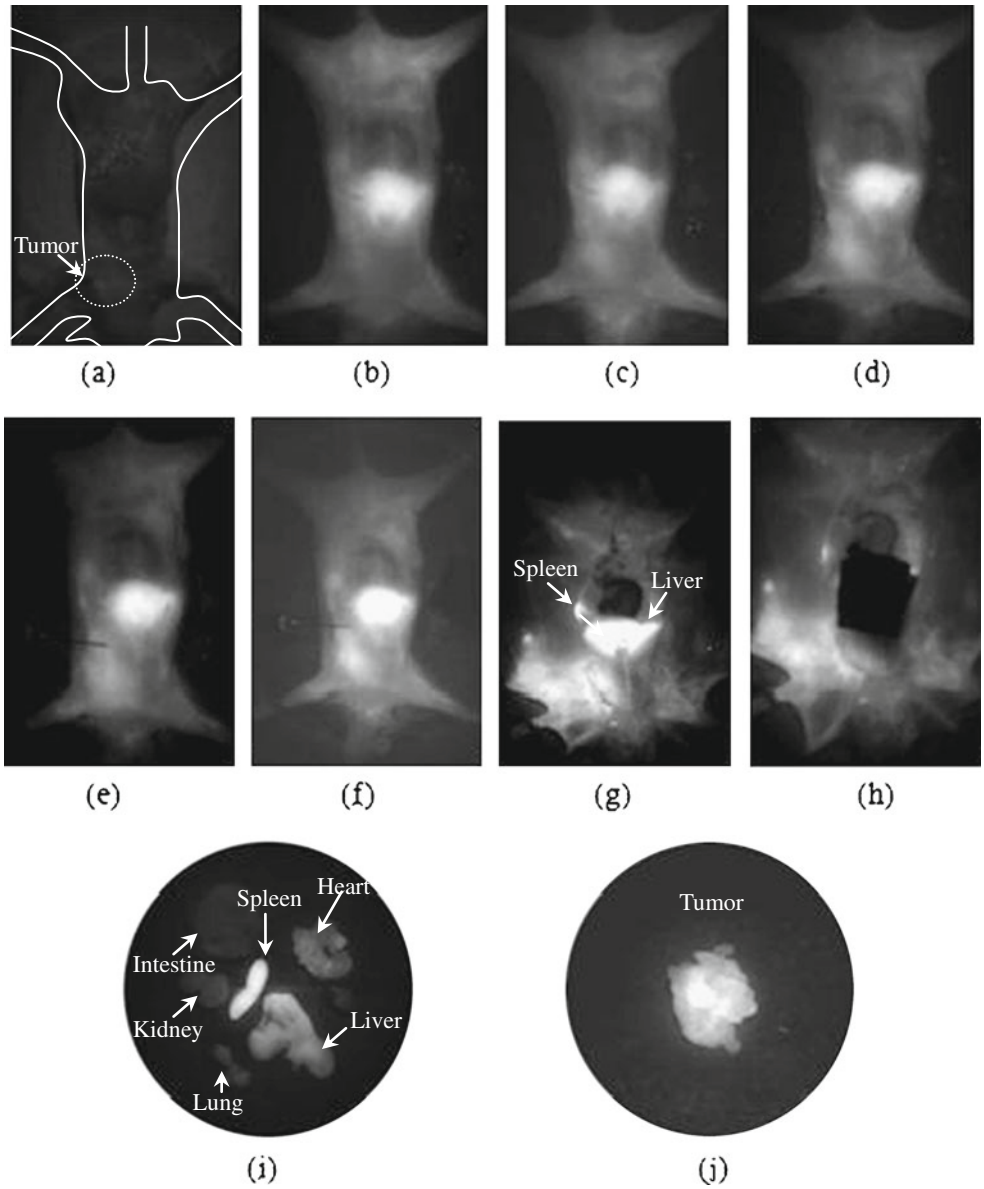

Fig. 7 A series fluorescence images of the mouse after folate-CdHgTe QDs was injected. **a** the fluorescent background measured by 765 nm excitation prior to QDs injection; **b** Fluorescence image of the same mouse approximately 1 min; **c** 5 min; **d** 1 h; **e** 2 h; **f** 5 h after folate-CdHgTe QDs conjugates was injected; **g** and **h** fluorescence image of the mouse taken after performing a thoracotomy; **i** The mouse was executed 6 h later. The major tissues of the mouse were removed and the fluorescence image was taken; **j** the tumor tissue of the mouse was removed and the fluorescence image was taken

penetration depth. The maximum emission wavelength of CdHgTe-folate conjugates in our experiment was 780 nm, which is in the region of 'near-infrared window', possessing maximum penetration depth and detection sensitivity of tissues.

Liu et al. [29] had investigated the cell viability of CdTe QDs and CdHgTe QDs, respectively. For CdHgTe QDs, a significant reduction in cell viability was observed even when tested at the low concentration (50 μM). It seemed that CdHgTe-folate conjugates (1.4 mM) were highly biocompatible and safe for further in vivo use. This data not only confirms the specific cytotoxicity of the probe towards the lung cancer cells, thereby highlighting its potential for concentration-dependent destruction of cancer in vitro and in vivo, but also justifies our safe strategy of their application for early tumor diagnosis.

To verify the affinity of folate and folate receptors in vitro, HeLa cells, due to FRs over-express on the their membranes, were incubated with CdHgTe-folate conjugates and CdHgTe QDs, respectively. The enhanced fluorescence

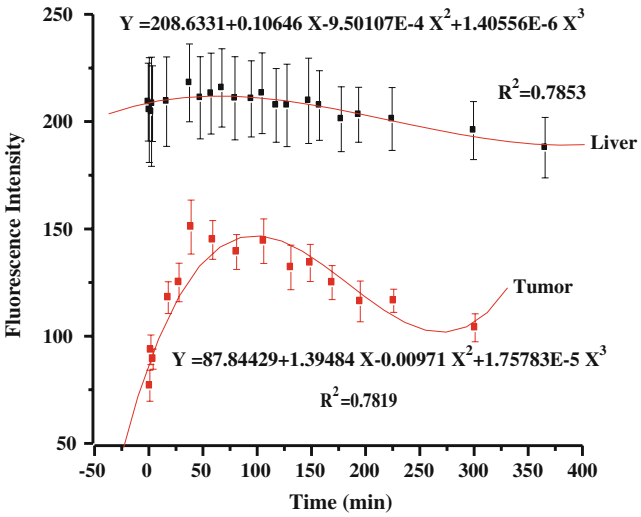

Fig. 8 Fluorescence intensities in tumor and liver tissues were collected at regular time intervals after CdHgTe-folate conjugates injected

signals within HeLa cells were attributed to the folate-mediated endocytosis of CdHgTe-folate conjugates. Hela cells incubating with CdHgTe QDs had weak fluorescence signals for nonspecific uptaking of nanoparticles in cancer cells. The imaging results demonstrated that CdHgTe-folate conjugates have high affinity to FRs and thus high target-specific to various cancer cells which are FRs positive.

For long time in vivo targeting imaging, CdHgTe-folate conjugates must have adequate stability and minimum nonspecific binding. No aggregation was observed for folic acid conjugation during the experimental time, which was attributed to high hydrophilicity and stability of CdHgTe-folate conjugates. Moreover, their fluorescence kept stable for a sufficiently long time in the conditions of ordinary temperature and light. Covalent bond between folic acid and QDs provide linking stability for these conjugates. Therefore, CdHgTe-folate conjugates could maintain the specificity to FRs in physiological condition.

In recent years, researchers mainly focused on real time tumor targeting and imaging. Cai et al [30] firstly reported the use of arginine-glycine-aspartic acid (RGD) peptide CdTe/ZnS QDs for in vivo tumor vasculature imaging. They demonstrated that the RGD peptide-labeled QDs could specifically target integrin $\alpha_v\beta_3$ of tumor vasculature in living mice. Folic acid was also used as tumor-targeting ligand for tumor imaging in this study. The experimental results showed the high and rapid accumulation of the injected conjugates, which indicated that the liver had the significantly nonspecific uptaking of the circulating conjugates in the mouse model. The main reason is that reticuloendothelial system (RES) acting as a part of the body's immune system concentrates mostly in the liver, spleen, lymph nodes and bone marrow. The mononuclear phagocytes in the RES are involved in the nonspecific uptake and clearance of nanoparticles.

CdHgTe-folate conjugates arrived to tumor tissue via blood vascular circulation and then penetrated from tumor vasculature to tumor cells. The majority of tumor cells over express the FRs which has high affinity to folate derivates. CdHgTe-folate conjugates were recognized by FRs on the membrane of tumor cells. As a result, these conjugates were delivered into tumor cells by FRs mediated endocytosis. Fluorescence signals in the tumor were detected as early as several minutes. As time extended, most CdHgTe-folate conjugates accumulating in tumor tissue caused fluorescence signal enhancing. The imaging results indicated that CdHgTe-folate conjugates could target to tumor tissue effectively. In addition, these conjugates were observed to maintain their fluorescence intensity more than 6 h after injection, which demonstrated their stability against physiological environment-induced degradation.

The nonspecific targeting must be decreased in the process of early tumor diagnosis. It was reported that hydrophilic polymers (such as PEG) coating with QDs could reduce the nonspecific uptake of RES [31]. PEG allowed greater vascular circulation time so that QDs could achieve targeting tissues efficiently rather than eliminating by RES. However, nonspecific uptake could not be avoided absolutely. CdHgTe-folate conjugates in this study also have significant nonspecific-uptaking by RES. More studies are needed to decrease the nonspecific effect of CdHgTe-folate conjugates and perform on the tumor targeting effect of this conjugates in other animal models.

Conclusion

In conclusion, due to the fact that the majority of tumor cells over express FRs, CdHgTe-folate conjugates have great potential to be utilized as a universal NIR fluorescence probe for detecting tumor in early phase. These conjugates synthesized in aqueous phase hold excellent optical properties, low photobleaching, deep tissue penetration and high imaging sensitivity for non-invasive imaging in vivo. CdHgTe-folate conjugates could specifically target to FRs both in vitro and in vivo. The results indicated that the conjugates offer new perspectives for imaging early diagnosis and monitoring of cancers.

Acknowledgement The authors are grateful to Natural Science Foundation Committee of China (NSFC81000666, NSFC81071194, NSFC30970776, NSFC30700779), the Ministry of Science and Technology (2009ZX09310-004), the Ministry of Education of China and China Pharmaceutical University for their financial supports.

References

1. Fottner C, Mettler E, Goetz M, Schirrmacher E, Anlauf M, Strand D, Schirrmacher R, Klöppel G, Delaney P, Schreckenberger M, Galle PR, Neurath MF, Kiesslich R, Weber MM (2010) In vivo molecular imaging of somatostatin receptors in pancreatic islet cells and neuroendocrine tumors by miniaturized confocal laser-scanning fluorescence microscopy. Endocrinology 151(5):2179–2188
2. Zhang J, Jia X, Lv XJ, Deng YL, Xie HY (2010) Fluorescent quantum dot-labeled aptamer bioprobes specifically targeting mouse liver cancer cells. Talanta 81(1–2):505–509
3. Davis SC, Samkoe KS, O'Hara JA, Gibbs-Strauss SL, Payne HL, Hoopes PJ, Paulsen KD, Pogue BW (2010) MRI-coupled fluorescence tomography quantifies EGFR activity in brain tumors. Acad Radiol 17(3):271–276
4. Do W, Hwang HY, Ko JH, Lee HK, Ryu SH, Song IC, Lee DS, Kim S (2010) A nucleolin-targeted multimodal nanoparticle imaging probe for tracking cancer cells using an aptamer. J Nucl Med 51(1):98–105
5. Ma J, Fan Q, Wang L, Jia N, Gu Z, Shen H (2010) Synthesis of magnetic and fluorescent bifunctional nanocomposites and their applications in detection of lung cancer cells in humans. Talanta 81(4–5):1162–1169
6. Boeneman K, Delehanty JB, Susumu K, Stewart MH, Medintz IL (2010) Intracellular bioconjugation of targeted proteins with semiconductor quantum dots. J Am Chem Soc 132(17):5975–5977
7. Hikage M, Gonda K, Takeda M, Kamei T, Kobayashi M, Kumasaka M, Watanabe M, Satomi S, Ohuchi N (2010) Nano-imaging of the lymph network structure with quantum dots. Nanotechnology 21(18):185103–185110
8. Lim YT, Noh YW, Cho JH, Han JH, Choi BS, Kwon J, Hong KS, Gokarna A, Cho YH, Chung BH (2009) Multiplexed imaging of therapeutic cells with multispectrally encoded magnetofluorescent nanocomposite emulsions. J Am Chem Soc 131(47):17145–17154
9. Zhang CY, Hu J (2010) Single quantum dot-based nanosensor for multiple DNA detection. Anal Chem 82(5):1921–1927
10. Xu H, Peng J, Tang HW, Li Y, Wu QS, Zhang ZL, Zhou G, Chen C, Li Y (2009) Hadamard transform spectral microscopy for single cell imaging using organic and quantum dot fluorescent probes. Analyst 134(3):504–511
11. Pan J, Liu Y, Feng SS (2010) Multifunctional nanoparticles of biodegradable copolymer blend for cancer diagnosis and treatment. Nanomedicine (Lond) 5(3):347–360
12. Gao J, Chen K, Xie R, Xie J, Yan Y, Cheng Z, Peng X, Chen X (2010) In vivo tumor-targeted fluorescence imaging using near-infrared non-cadmium quantum dots. Bioconjug Chem 21(4):604–609
13. Li Z, Huang P, Zhang X, Lin J, Yang S, Liu B, Gao F, Xi P, Ren Q, Cui D (2010) RGD-conjugated dendrimer-modified gold nanorods for in vivo tumor targeting and photothermal therapy. Mol Pharm 7(1):94–104
14. Hwang SY, Cho do Y, Kim HK, Cho SH, Choo J, Yoon WJ, Lee EK (2010) Preparation of targeting proteoliposome by post-insertion of a linker molecule conjugated with recombinant human epidermal growth factor. Bioconjug Chem 21(2):345–351
15. Chrastina A, Valadon P, Massey KA, Schnitzer JE (2010) Lung vascular targeting using antibody to aminopeptidase P: CT-SPECT imaging, biodistribution and pharmacokinetic analysis. J Vasc Res 47(6):531–543
16. Kularatne SA, Low PS (2010) Targeting of nanoparticles: folate receptor. Methods Mol Biol 624:249–265
17. Kamen BA, Capdevila A (1986) Receptor-mediated folate accumulation is regulated by the cellular folate content. Proc Natl Acad Sci 83:5983–5987
18. Ke JH, Lin JJ, Carey JR, Chen JS, Chen CY, Wang LF (2010) A specific tumor-targeting magnetofluorescent nanoprobe for dual-modality molecular imaging. Biomaterials 31(7):1707–1715
19. Zhang J, Deng D, Qian Z, Liu F, Chen X, An L, Gu Y (2010) The targeting behavior of folate-nanohydrogel evaluated by near infrared imaging system in tumor-bearing mouse model. Pharm Res 27(1):46–55
20. Fan L, Li F, Zhang H, Wang Y, Cheng C, Li X, Gu CH, Yang Q, Wu H, Zhang S (2010) Co-delivery of PDTC and doxorubicin by multifunctional micellar nanoparticles to achieve active targeted drug delivery and overcome multidrug resistance. Biomaterials 31 (21):5634–5642
21. Yoo HS, Park TG (2004) Folate-receptor-targeted delivery of doxorubicin nano-aggregates stabilized by doxorubicin–PEG–folate conjugate. J Control Release 100(2):247–256
22. Zhang L, Xia J, Zhao Q, Liu L, Zhang Z (2010) Functional graphene oxide as a nanocarrier for controlled loading and targeted delivery of mixed anticancer drugs. Small 6(4):537–544
23. Liu F, Deng D, Chen X, Qian Z, Achilefu S, Gu Y (2010) Folate-polyethylene glycol conjugated near-infrared fluorescence probe with high targeting affinity and sensitivity for in vivo early tumor diagnosis. Mol Imaging Biol Apr 8. [Epub ahead of print]
24. Gu B, Xie C, Zhu J, He W, Lu W (2010) Folate-PEG-CKK(2)-DTPA, a potential carrier for lymph-metastasized tumor targeting. Pharm Res 27(5):933–942
25. Kularatne SA, Low PS (2010) Targeting of nanoparticles: folate receptor. Methods Mol Biol 624:249–265
26. Retnakumari A, Setua S, Menon D, Ravindran P, Muhammed H, Pradeep T, Nair S, Koyakutty M (2010) Molecular-receptor-specific, non-toxic, near-infrared-emitting Au cluster-protein nanoconjugates for targeted cancer imaging. Nanotechnology 21 (5):055103–055109
27. Mohapatra S, Mallick SK, Maiti TK, Ghosh SK, Pramanik P (2007) Synthesis of highly stable folic acid conjugated magnetite nanoparticles for targeting cancer cells. Nanotechnology 18:385102–385111
28. Chen H, Wang Y, Xu J, Ji J, Zhang J, Hu Y, Gu Y (2008) Non-invasive near infrared fluorescence imaging of CdHgTe quantum dots in mouse model. J Fluoresc 18(15):801–811
29. Liu L, Zhang J, Su X, Mason PP (2008) Mason in vitro and in vivo assessment of CdTe and CdHgTe toxicity and clearance. J Biomed Nanotechnol 24(4):524–528
30. Cai WB, Shin DW, Chen K, Gheysens O, Cao Q, Wang SX, Gambhir SS, Chen X (2006) Peptide-labeled near-infrared quantum dots for imaging tumor vasculature in living subjects. Nano Lett 6(4):669–676
31. Akerman ME, Chan WCW, Laakkonen P, Bhatia SN, Ruoslahti E (2002) Nanocrystal targeting in vivo. Proc Natl Acad Sci 99 (20):12617–12621